

SYSTEM IDENTIFICATION OF SMALL-SCALE HELICOPTER VIA EKF WITH DATA-DRIVEN NOISE COVARIANCE DETERMINATION

Eunjung Kim[1†], Bin Seo[1], Seungkeun Kim[1] & Jinyoung Suk[1‡]

[1]Department of Aerospace Engineering, Chungnam National University, Daejeon, Republic of Korea

Abstract

This paper performs system identification of a small-scale helicopter using an Extended Kalman Filter (EKF). The dynamic model is formulated using 6-Degree-of-Freedom (6-DOF) rigid-body equations of motion. To facilitate system identification, a tailored EKF framework is designed. EKF noise covariance matrices are determined from flight data collected during hovering conditions. Utilizing these noise covariance matrices, helicopter system identification is conducted. The identified model, established based on the tuned noise covariance matrices, is validated through numerical simulations. Furthermore, dynamic modes and dynamic characteristics of the identified small-scale helicopter model are analyzed.

Keywords: Small-scale Helicopter, System Identification, Extended Kalman Filter, Noise Covariance Matrix

1. Introduction

Small-scale helicopters are widely utilized in the field of Unmanned Aerial Vehicles (UAVs) due to their high maneuverability and operational flexibility. Although their flight speed is slower than that of fixed-wing UAVs, their vertical takeoff and landing (VTOL) capability enables hovering and low-observability characteristics, making them highly suitable for reconnaissance missions. However, most helicopter systems tend to be relatively unstable and exhibit lower control performance compared to fixed-wing UAVs. Due to the complex dynamic characteristics of helicopters, which include aerodynamic interference and cross-axis coupling, obtaining an accurate mathematical model required for model analysis is a challenging task. Furthermore, their small size renders them highly vulnerable to external disturbances. Consequently, a precise dynamic model is essential to accurately understand the characteristics of small-scale helicopters and to design high-performance flight controllers. In this paper, offline system identification is performed using an Extended Kalman Filter (EKF) to estimate the stability and control derivatives, which are key flight parameters of a small-scale helicopter. The target platform used for identification is the 'Align T-Rex 300X Helicopter System' shown in Fig. 1. This system is equipped with a PX4-based PixHawk 6c Mini Flight Control Computer (FCC), and flight tests are conducted in a closed-loop system configuration where only a P-controller is applied at a level sufficient to ensure stable control. To enhance the accuracy of EKF-based system identification, we propose a methodology for configuring the EKF noise covariance matrices (Q and R) by analyzing flight data obtained from a hovering state. Subsequently, system identification is conducted using flight data that includes frequency sweeps. The identified 6-DOF model is validated through an axis-by-axis comparison between the conventional EKF identification method and the proposed EKF approach. Furthermore, to validate the identified model, simulations are performed by applying the exact control inputs used during the identification process, and the corresponding results are analyzed. In future work, the Active Disturbance Rejection Control (ADRC) technique will be applied to the identified small-scale helicopter model to estimate and compensate for disturbances in real time, followed by an in-depth analysis of attitude control in the hovering state.

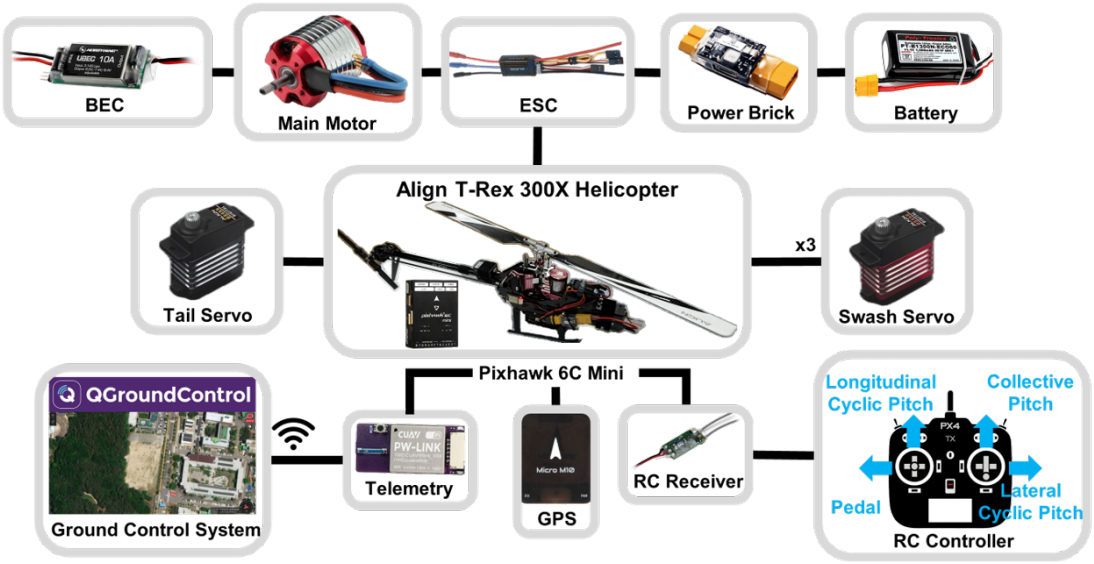


Figure 1 – Helicopter System.

2. System Dynamic Model

The helicopter motion is described in the body-fixed coordinate system using the 6-DOF rigid-body equations of motion. The corresponding body-fixed axis convention is shown in Fig. 2.

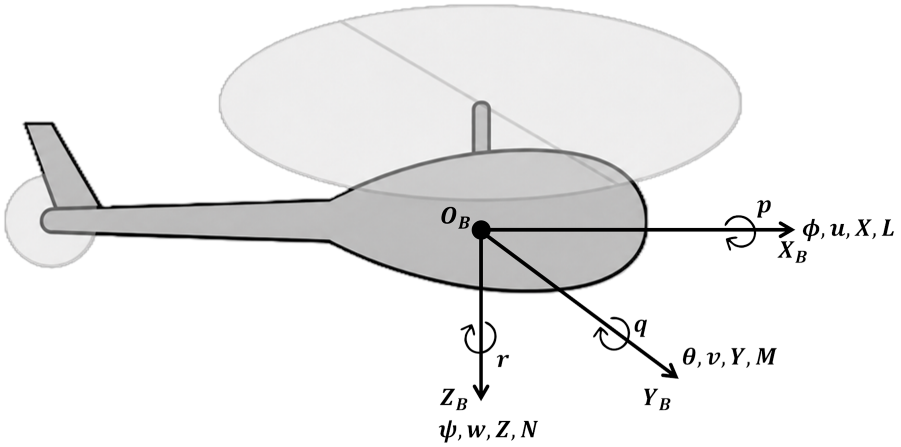


Figure 2 – Body-fixed coordinate system of the helicopter.

For small perturbations about a trim condition, the translational dynamics can be expressed as:

$$\begin{aligned} \dot{u} &= \frac{X}{m} - w_0 q + v_0 r - g\cos\Theta_0\,\theta \\ \dot{v} &= \frac{Y}{m} - u_0 r + w_0 p + g\cos\Theta_0\,\phi \\ \dot{w} &= \frac{Z}{m} - v_0 p + u_0 q - g\sin\Theta_0\,\theta \end{aligned} \tag{1}$$

Where, u, v, and w are the body-axis velocity perturbations, p, q, and r are the angular rates, X, Y, and Z denote the body-axis forces, m is the mass, g is the gravitational acceleration, and the subscript 0 denotes the trim condition. Assuming that the body-fixed axes are aligned with the principal inertia

axes, the rotational dynamics for the angular rates are given by:

$$\begin{aligned}\dot{p} &= \frac{L}{I_{xx}} + \frac{I_{yy}-I_{zz}}{I_{xx}}qr \\ \dot{q} &= \frac{M}{I_{yy}} + \frac{I_{zz}-I_{xx}}{I_{yy}}pr \\ \dot{r} &= \frac{N}{I_{zz}} + \frac{I_{xx}-I_{yy}}{I_{zz}}pq\end{aligned} \tag{2}$$

where L, M, and N are the rolling, pitching, and yawing moments, respectively, and I_{xx}, I_{yy}, and I_{zz} are the moments of inertia about the body axes. By applying a first-order Taylor expansion about the trim condition, the force and moment terms are represented using stability and control derivatives. The full-state vector and control input vector are defined as:

$$\begin{aligned}\mathbf{x} &= \begin{bmatrix} u & v & w & p & q & r & \theta & \phi \end{bmatrix}^T \\ \mathbf{u} &= \begin{bmatrix} \delta_{lon} & \delta_{lat} & \delta_{ped} & \delta_{coll} \end{bmatrix}^T\end{aligned} \tag{3}$$

The resulting linearized full-state model is expressed as:

$$\begin{aligned}\dot{\mathbf{x}} &= \mathbf{A}\mathbf{x} + \mathbf{B}\mathbf{u} \\ \mathbf{y} &= \mathbf{C}\mathbf{x} + \mathbf{D}\mathbf{u}\end{aligned} \tag{4}$$

The full-state stability derivative matrix is given by:

$$\mathbf{A} = \begin{bmatrix} X_u & X_v & X_w & X_p & X_q & X_r & -g & 0 \\ Y_u & Y_v & Y_w & Y_p & Y_q & Y_r & 0 & g \\ Z_u & Z_v & Z_w & Z_p & Z_q & Z_r & 0 & 0 \\ L_u & L_v & L_w & L_p & L_q & L_r & 0 & 0 \\ M_u & M_v & M_w & M_p & M_q & M_r & 0 & 0 \\ N_u & N_v & N_w & N_p & N_q & N_r & 0 & 0 \\ 0 & 0 & 0 & 0 & 1 & 0 & 0 & 0 \\ 0 & 0 & 0 & 1 & 0 & 0 & 0 & 0 \end{bmatrix} \tag{5}$$

The corresponding control derivative matrix is:

$$\mathbf{B} = \begin{bmatrix} X_{\delta_{lon}} & X_{\delta_{lat}} & X_{\delta_{ped}} & X_{\delta_{coll}} \\ Y_{\delta_{lon}} & Y_{\delta_{lat}} & Y_{\delta_{ped}} & Y_{\delta_{coll}} \\ Z_{\delta_{lon}} & Z_{\delta_{lat}} & Z_{\delta_{ped}} & Z_{\delta_{coll}} \\ L_{\delta_{lon}} & L_{\delta_{lat}} & L_{\delta_{ped}} & L_{\delta_{coll}} \\ M_{\delta_{lon}} & M_{\delta_{lat}} & M_{\delta_{ped}} & M_{\delta_{coll}} \\ N_{\delta_{lon}} & N_{\delta_{lat}} & N_{\delta_{ped}} & N_{\delta_{coll}} \\ 0 & 0 & 0 & 0 \\ 0 & 0 & 0 & 0 \end{bmatrix} \tag{6}$$

The coefficients in $\mathbf{A}$ are the stability derivatives, whereas the coefficients in $\mathbf{B}$ are the control derivatives to be identified from flight data. This full-state formulation provides the target model structure for the complete identification process. For preliminary algorithm verification, the model is reduced into longitudinal and lateral-directional subsystems in the following section.

3. Helicopter System Identification Based on Extended Kalman Filter

In this study, system identification is conducted for the Align T-Rex 300X, a small-scale helicopter system shown in Fig. 1. The proposed identification algorithm is first verified using reduced longitudinal and lateral-directional models extracted from the full-state formulation in Eq. (4). The same framework is then formulated for full-state identification using flight data collected during hovering and frequency-sweep maneuvers.

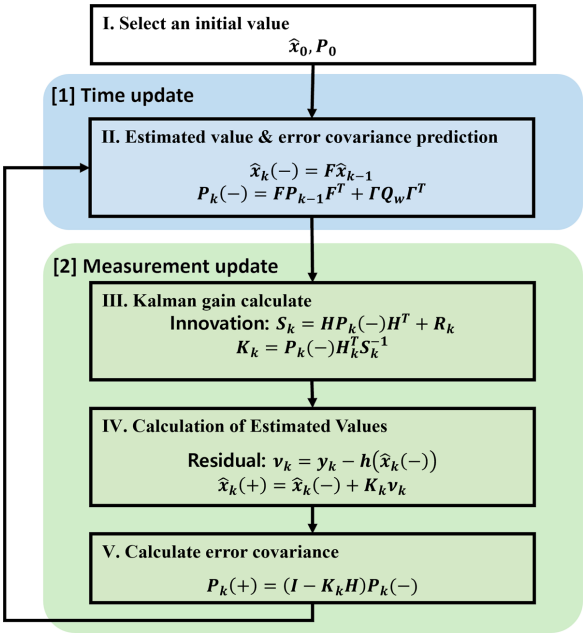


Figure 3 – EKF-based offline parameter estimation procedure.

3.1 Mathematical Modeling and State Augmentation

To establish a reliable identification framework, this study adopts the 6-DOF rigid-body equations of motion as detailed in [1]. In this preliminary study, the identification is performed by decoupling dynamics into longitudinal and lateral-directional models. The state vector $\mathbf{x}$ and input vector $\mathbf{u}$ for each axis are defined as:

$$\mathbf{x}_{lon} = \begin{bmatrix} u & w & q & \theta \end{bmatrix}^T, \quad \mathbf{u}_{lon} = \begin{bmatrix} \delta_{lon} \end{bmatrix} \tag{7}$$

$$\mathbf{x}_{lat} = \begin{bmatrix} v & p & r & \phi \end{bmatrix}^T, \quad \mathbf{u}_{lat} = \begin{bmatrix} \delta_{lat} \end{bmatrix} \tag{8}$$

The aerodynamic characteristics for each axis are extracted into separate parameter vectors to be identified:

$$\beta_{lon} = \begin{bmatrix} X_u & X_w & X_q & Z_u & Z_w & Z_q & M_u & M_w & M_q & X_{\delta_{lon}} & Z_{\delta_{lon}} & M_{\delta_{lon}} \end{bmatrix}^T \tag{9}$$

$$\beta_{lat} = \begin{bmatrix} Y_v & Y_p & Y_r & L_v & L_p & L_r & N_v & N_p & N_r & Y_{\delta_{lat}} & L_{\delta_{lat}} & N_{\delta_{lat}} \end{bmatrix}^T \tag{10}$$

The system is formulated into an augmented state-space model by combining the dynamic states and aerodynamic derivative parameters:

$$\mathbf{x}_{aug} = \begin{bmatrix} \mathbf{x} \\ \beta \end{bmatrix} \tag{11}$$

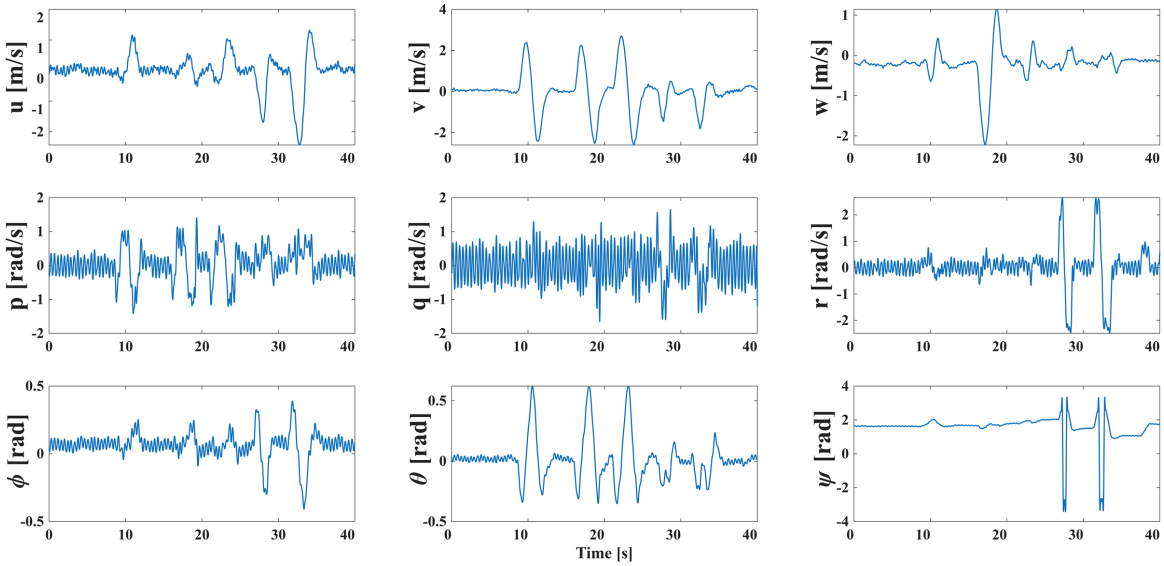
Under the assumption that these derivatives remain constant during the identification interval, the augmented system is expressed as:

$$\begin{bmatrix} \dot{\mathbf{x}} \\ \dot{\beta} \end{bmatrix} = \begin{bmatrix} f(\mathbf{x}, \mathbf{u}, \beta) \\ \mathbf{0} \end{bmatrix} + \begin{bmatrix} \omega \\ \mathbf{0} \end{bmatrix} \tag{12}$$

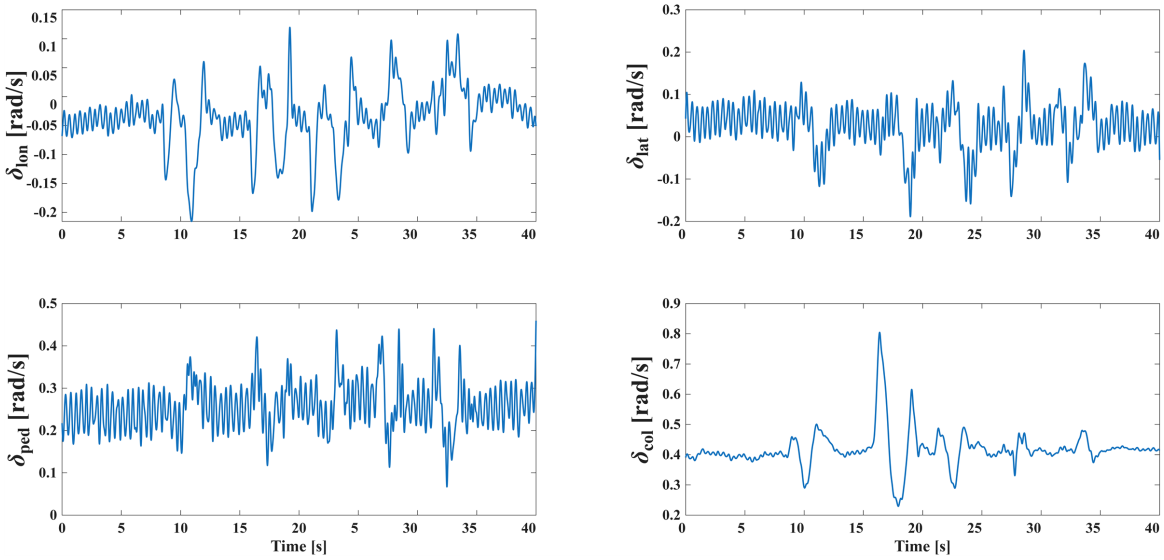
where $f(\mathbf{x}, \mathbf{u}, \beta)$ denotes the state transition function, and the constant coefficients in [1] are replaced by the elements of β for estimation. This decoupled identification step is used as an intermediate verification stage before applying the same EKF framework to the full-state model.

3.2 Flight Data Configuration for Full-State Identification

After verifying the EKF framework using the reduced longitudinal and lateral-directional models, the same identification procedure is extended to the full-state helicopter model. For this purpose, the flight-log data are organized into the full-state response vector and the four actuator command inputs. The measured state histories and the corresponding control input histories are shown in Fig. 4.



(a) Measured state responses.



(b) Actuator command inputs.

Figure 4 – Flight data used for full-state identification.

At each sampled time instant, the data are arranged using the state and input order defined in Eq. (3):

$$\mathbf{x}_k = \begin{bmatrix} u_k & v_k & w_k & p_k & q_k & r_k & \theta_k & \phi_k \end{bmatrix}^T, \quad u_k = \begin{bmatrix} \delta_{lon,k} & \delta_{lat,k} & \delta_{ped,k} & \delta_{coll,k} \end{bmatrix}^T \tag{13}$$

where $\mathbf{x}_k$ is the measured full-state vector and δ_k is the actuator input vector. Unlike the reduced longitudinal and lateral-directional cases, the full-state formulation uses all four control channels simultaneously and preserves the cross-axis coupling terms in the state-space model.

The full-state augmented vector is defined by combining the measured state vector with the unknown stability and control derivative vector:

$$\begin{aligned} \mathbf{x}_{aug,full} &= \begin{bmatrix} \mathbf{x}^T & \beta^T \end{bmatrix}^T, \\ \beta &= \begin{bmatrix} X_u & X_v & \cdots & N_{\delta_{coll}} \end{bmatrix}^T \end{aligned} \tag{14}$$

where β contains the full-state aerodynamic derivatives to be identified. Under the constant-derivative assumption, the continuous augmented dynamics are expressed as:

$$\begin{bmatrix} \dot{\mathbf{x}} \\ \dot{\beta} \end{bmatrix} = \begin{bmatrix} \mathbf{A}(\beta)\mathbf{x} + \mathbf{B}(\beta)\delta \\ \mathbf{0} \end{bmatrix} + \begin{bmatrix} \omega_x \\ \mathbf{0} \end{bmatrix} \tag{15}$$

where ω_x represents the process uncertainty associated with the full-state dynamics.

3.3 EKF-Based Offline Parameter Estimation

The system identification utilizes an offline EKF framework based on the continuous augmented dynamics in Eq. (15). EKF estimates the state and parameter vector simultaneously by repeating a prediction-correction process over the recorded flight data [2].

In the prediction step, the augmented state estimate and the error covariance are propagated using the full-state model. In the correction step, the predicted response is updated using the measured flight data. The full-state measurement equation is given by:

$$\mathbf{y}_{f,k} = \mathbf{H}_f \mathbf{X}_{aug,full,k} + v_k, \quad \mathbf{H}_f = \begin{bmatrix} \mathbf{I}_8 & \mathbf{0}_{8\times n_\beta} \end{bmatrix} \tag{16}$$

where n_β is the number of identified parameters in β and v_k is the measurement noise. The measurement update directly corrects the physical state components, while the aerodynamic derivatives are updated through the state-parameter covariance. By minimizing the residual between the predicted and measured flight responses, the EKF iteratively converges to the identified stability and control derivatives.

3.4 Determination of Noise Covariance via Hovering Data

The identification performance of the EKF is highly dependent on the tuning of the noise covariance matrices Q and R. In this study, the measurement noise covariance R is determined by analyzing the frequency-domain characteristics of hovering flight data. According to the spectral analysis theory presented in [3], the variance of a signal in the time domain is equivalent to the integral of its autospectrum over the frequency range:

$$\sigma_x^2 = \int_0^\infty G_{xx}(f)\, df = \frac{1}{N-1} \sum_{n=1}^{N} (x_n - x_{ave})^2 \tag{17}$$

where $G_{xx}(f)$ is the autospectrum of the measured signal. For small-scale helicopters, the rigid-body maneuvering dynamics are primarily concentrated in the low-frequency region, typically below 5–10 Hz, whereas high-frequency components are dominated by structural vibrations and sensor noise. To isolate the pure sensor and vibration noise from the actual vehicle motion, the measurement noise σ_i^2 for each axis was calculated by integrating the power spectral density (PSD) over the frequency range above 15 Hz. This frequency-based noise definition ensures that the R matrix accurately represents stochastic uncertainty without including the helicopter's inherent dynamics. Accordingly, R is defined separately for the decoupled and full-state models:

$$R_{lon} = \mathrm{diag}(\sigma_u^2, \sigma_w^2, \sigma_q^2, \sigma_\theta^2) \tag{18}$$

$$R_{lat} = \mathrm{diag}(\sigma_v^2, \sigma_p^2, \sigma_r^2, \sigma_\phi^2) \tag{19}$$

$$R_{full} = \mathrm{diag}(\sigma_u^2, \sigma_v^2, \sigma_w^2, \sigma_p^2, \sigma_q^2, \sigma_r^2, \sigma_\theta^2, \sigma_\phi^2) \tag{20}$$

The system noise covariance matrix Q accounts for model uncertainties for the parameter vector β. The corresponding elements in Q are set to zero to reflect the constant derivative assumption:

$$Q = \mathrm{diag}\left([\sigma_{x,state}^2, \sigma_\beta^2] \right), \quad \sigma_\beta^2 = 0 \tag{21}$$

4. Identification Results

4.1 Longitudinal and Lateral Identification Results

The identification results confirm that the hover-based Q and R tuning significantly improves the EKF prediction performance. Figs. 5–6 compare the measured flight states with the Kalman-filter-predicted states obtained during the identification process. The proposed covariance tuning enables the predicted states to follow the measured responses more closely, whereas the baseline EKF tends to overly smooth the signals due to high-level rotor vibrations. Therefore, these results demonstrate improved prediction capability during parameter estimation, rather than serving as an independent validation of the identified model.

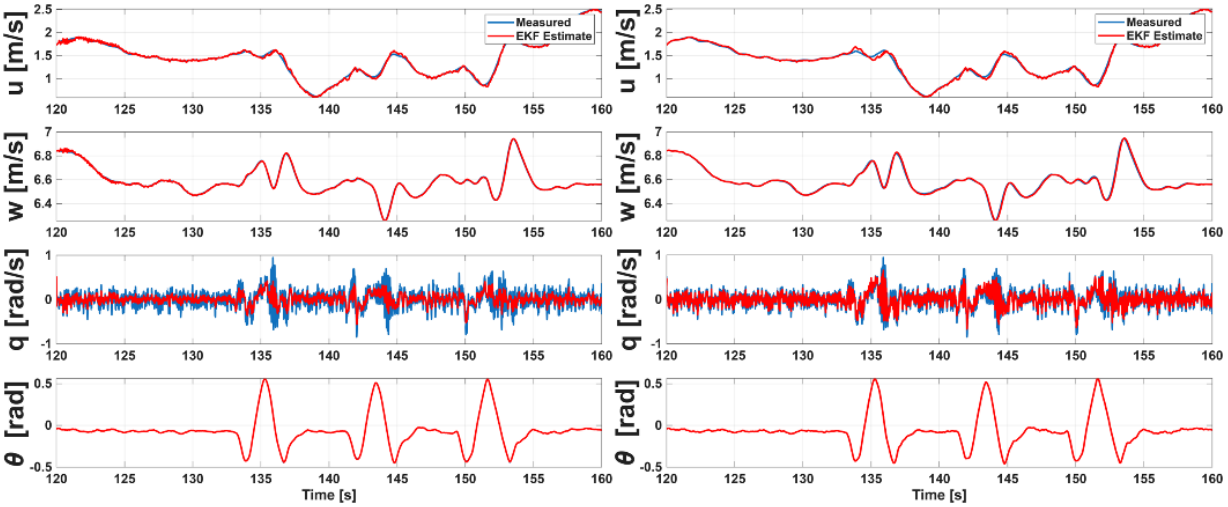


Figure 5 – Longitudinal EKF prediction result (left: sensor noise only, right: proposed method).

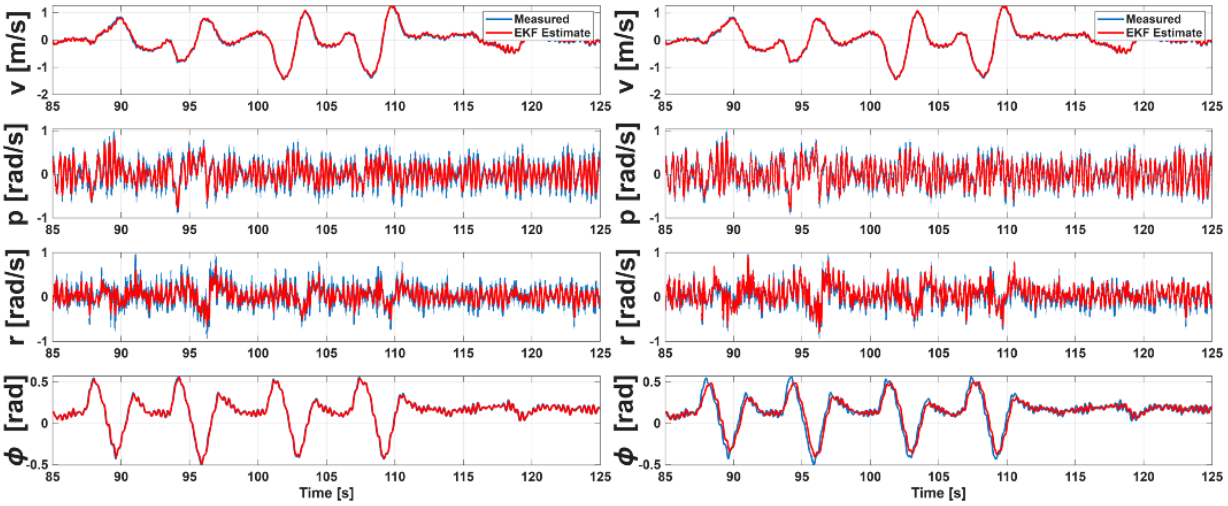


Figure 6 – Lateral EKF prediction result (left: sensor noise only, right: proposed method).

From the converged parameters, the identified numerical state-space models for the T-Rex 300X are obtained as follows.

Longitudinal model

$$\begin{bmatrix} \dot{u} \\ \dot{w} \\ \dot{q} \\ \dot{\theta} \end{bmatrix} = \begin{bmatrix} -1.3108 & 0.2167 & 28.0140 & -9.81 \\ -0.1075 & 0.0247 & 0.7953 & 0 \\ 0.7870 & -0.2279 & -14.3137 & 0 \\ 0 & 0 & 1 & 0 \end{bmatrix} \begin{bmatrix} u \\ w \\ q \\ \theta \end{bmatrix} + \begin{bmatrix} 1.3259 \\ 0.1850 \\ -2.7221 \\ 0 \end{bmatrix} \delta_{lon} \tag{22}$$

Lateral model

$$\begin{bmatrix} \dot{v} \\ \dot{p} \\ \dot{r} \\ \dot{\phi} \end{bmatrix} = \begin{bmatrix} 1.1819 & -2.6550 & -6.0232 & 9.81 \\ 3.5744 & -8.2497 & -0.9134 & 0 \\ -1.6546 & 2.7705 & -1.9302 & 0 \\ 0 & 1 & 0 & 0 \end{bmatrix} \begin{bmatrix} v \\ p \\ r \\ \phi \end{bmatrix} + \begin{bmatrix} -3.3376 \\ 1.2602 \\ -0.8608 \\ 0 \end{bmatrix} \delta_{lat} \tag{23}$$

The physical validity of the identified model was verified using the pole-zero map illustrated in Fig. 7, which reveals the fundamental rotorcraft modes.

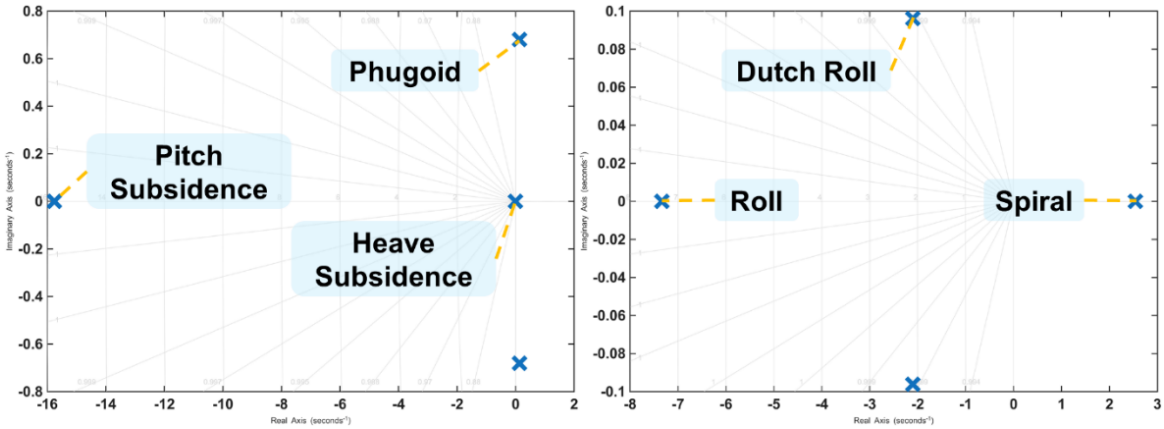


Figure 7 – Pole-zero maps of the reduced longitudinal and lateral models.

To provide a quantitative evaluation of the identified dynamics, the specific dynamic-mode parameters, including poles, natural frequencies, and damping ratios, are summarized in Table 1.

Table 1 – Dynamic Mode Analysis of the Reduced Models

Axis	***Dynamic Mode***	***Pole***	***Natural Frequency***	***Damping Ratio*** (ζ)
Longitudinal	Phugoid	$0.133 + 0.681i$	$0.693\ (\mathrm{rad/s})$	-0.191
	Pitch Subsidence	-15.8	$15.8\ (\mathrm{rad/s})$	1
	Heave Subsidence	-0.00655	$0.00655\ (\mathrm{rad/s})$	1
Lateral	Dutch Roll	$-2.1 + 0.0961i$	$2.1\ (\mathrm{rad/s})$	0.999
	Roll	-7.33	$7.33\ (\mathrm{rad/s})$	1
	Spiral	2.54	$2.54\ (\mathrm{rad/s})$	-1

The longitudinal dynamics exhibit well-defined pitch subsidence, heave subsidence, and phugoid modes. The lateral dynamics exhibit roll, Dutch-roll, and spiral modes [4, 5]. These identified dynamic-mode characteristics are highly consistent with the known flight properties of small-scale helicopters. In particular, the high natural frequency of the roll mode and the characteristic oscillations of the phugoid and Dutch-roll modes confirm that the identified A matrix in Eqs. (22) and (23) accurately captures the essential rigid-body motion of the T-Rex 300X.

4.2 Full-State Identification Results

The full-state identification performance is evaluated using the Variance Accounted For (VAF), which is defined for each output channel as:

$$\mathrm{VAF}_i = \left[1 - \frac{\mathrm{var}\,(y_i - \hat{y}_i)}{\mathrm{var}\,(y_i)}\right] \times 100\ (\%) \tag{24}$$

where y_i and $\hat{y}_i$ denote the measured and predicted responses of the i-th state, respectively. In this metric, a value close to 100% indicates that most of the measured variance is reproduced by the identified model, whereas a low or negative value indicates that the residual error variance is comparable to, or larger than, the variance of the measured response. Because the VAF is normalized by the variance of each measured channel, it provides a convenient basis for comparing states with different physical units, such as translational velocities, angular rates, and attitude angles. However, VAF should be interpreted together with the dynamic mode analysis, since a high time-response fit does not necessarily guarantee that the identified state matrix preserves physically meaningful rotorcraft modes. The full-state VAF result is shown in Fig. 8, providing a channel-wise measure of the identified model's prediction accuracy.

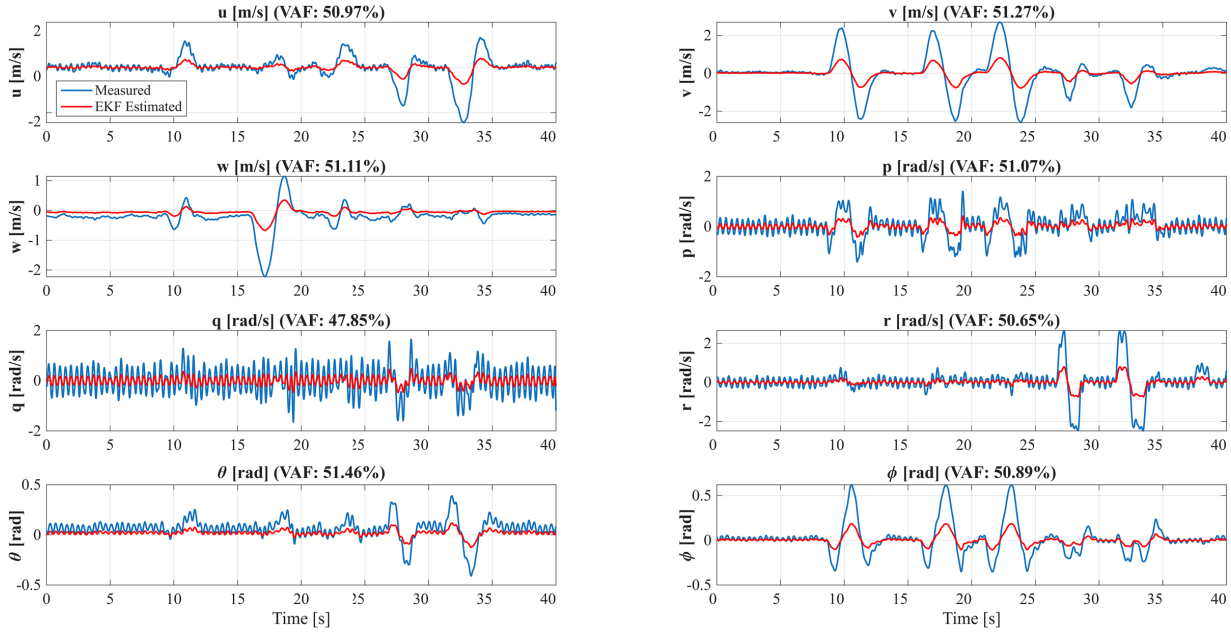


Figure 8 – Full-state identification result evaluated using VAF.

From the converged parameters, the identified numerical state-space models for the T-Rex 300X are obtained as follows.

Full-state model

$$\begin{bmatrix} \dot{u} \\ \dot{v} \\ \dot{w} \\ \dot{p} \\ \dot{q} \\ \dot{r} \\ \dot{\theta} \\ \dot{\phi} \end{bmatrix} = \begin{bmatrix} 0.3 & 0.38 & 0.05 & 0 & 1.53 & 0 & -9.81 & 0 \\ -0.723 & 0.21 & 0 & -0.267 & 0 & -1.75 & 0 & 9.81 \\ -0.033 & 0 & -0.26 & 0 & -0.0383 & 0 & 0 & 0 \\ -0.24 & 0.456 & -0.17 & -7.165 & 0.386 & -0.012 & 0 & 0 \\ -0.002 & 0.015 & -0.003 & 0 & -0.52 & 0 & 0 & 0 \\ 0 & 0.224 & 0.046 & -0.12 & 0 & -0.54 & 0 & 0 \\ 0 & 0 & 0 & 0 & 1 & 0 & 0 & 0 \\ 0 & 0 & 0 & 1 & 0 & 0 & 0 & 0 \end{bmatrix} \begin{bmatrix} u \\ v \\ w \\ p \\ q \\ r \\ \theta \\ \phi \end{bmatrix} + \begin{bmatrix} -0.4864 & 0 & 0 & 0 \\ 0 & 0.3528 & -0.002 & 0 \\ 0 & 0 & 0 & -0.44 \\ 0.067 & 0.02 & 0 & 0 \\ 0.001 & 0.008 & 0 & 0 \\ 0 & 0.02 & 0.1 & 0.01 \\ 0 & 0 & 0 & 0 \\ 0 & 0 & 0 & 0 \end{bmatrix} \begin{bmatrix} \delta_{lon} \\ \delta_{lat} \\ \delta_{ped} \\ \delta_{coll} \end{bmatrix} \tag{25}$$

The pole-zero map of the full-state identified model will be used to analyze the coupled dynamic modes.

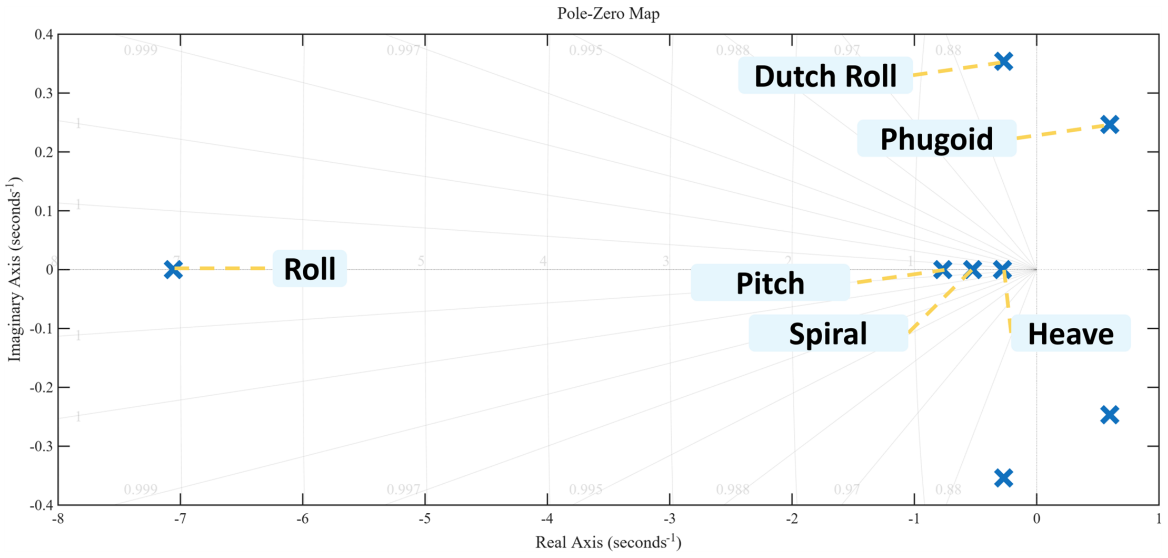


Figure 9 – Pole-zero map of the full-state identified model.

The corresponding full-state dynamic-mode parameters are summarized in Table 2.

Table 2 – Dynamic Mode Analysis of the Full-State Identified Model

Axis	*Dynamic Mode*	*Pole*	*Natural Frequency*	*Damping Ratio* (ζ)
Full-State	Roll Mode	-7.06	$7.06\ (\mathrm{rad/s})$	1
	Pitch Mode	-0.77	$0.77\ (\mathrm{rad/s})$	1
	Spiral Mode	-0.52	$0.52\ (\mathrm{rad/s})$	1
	Heave Mode	-0.28	$0.28\ (\mathrm{rad/s})$	1
	Dutch Roll	$-0.269 \pm 0.354i$	$0.445\ (\mathrm{rad/s})$	0.605
	Phugoid	$0.598 \pm 0.247i$	$0.647\ (\mathrm{rad/s})$	-0.924

5. Conclusion

This paper proposed a systematic EKF identification framework for a small-scale helicopter, based on spectral-based noise determination. By deriving Q and R from the 15 Hz spectral analysis of hovering data, the need for conventional heuristic tuning was eliminated. The results demonstrated that the proposed method effectively captures rigid-body dynamics while distinguishing high-frequency sensor noise. Validation through dynamic mode analysis confirmed the high fidelity of the identified state-space model in representing the physical flight characteristics of the T-Rex 300X. These results will serve as a reliable baseline for future work involving the design and simulation of an ADRC-based flight control system.

6. Contact Author Email Address

‡: jsuk@cnu.ac.kr (corresponding author)
†: kej000418@o.cnu.ac.kr

7. Copyright Statement

The authors confirm that they, and/or their company or organization, hold copyright on all of the original material included in this paper. The authors also confirm that they have obtained permission, from the copyright holder of any third party material included in this paper, to publish it as part of their paper. The authors confirm that they give permission, or have obtained permission from the copyright holder of this paper, for the publication and distribution of this paper as part of the ICAS proceedings or as individual off-prints from the proceedings.

Acknowledgment

This work was supported by the Korea Research Institute for Defense Technology Planning and Advancement (KRIT) grant funded by the Defense Acquisition Program Administration (DAPA) and Daejeon Metropolitan City (Daejeon Defense Industry Innovation Cluster Project, No. DC2022RL).

References

[1] K. Bang, N. Kim, C. Hong, and J. Suk. Parameter estimation of a small-scale unmanned helicopter by automated flight test method. *Journal of Institute of Control, Robotics and Systems*, 14(9):916–924, 2008.

[2] R. E. Kalman. Contributions to the theory of optimal control. *Bol. Soc. Mat. Mexicana*, pages 102–119, 1960.

[3] Mark B. Tischler and Robert K. Remple. *Aircraft and rotorcraft system identification: engineering methods with flight test examples*. American Institute of Aeronautics and Astronautics, Inc., 2012.

[4] C. Venkatesan. *Fundamentals of helicopter dynamics*. CRC Press, 2014.

[5] Gareth D. Padfield. *Helicopter flight dynamics: including a treatment of tiltrotor aircraft*. John Wiley & Sons, 2018.